IV International Conference on Computational Methods for Coupled Problems in Science and Engineering
COUPLED PROBLEMS 2011
M. Papadrakakis, E. Oñate and B. Schrefler (Eds)

HIERARCHICAL HYBRID SIMULATION OF BIOFILM GROWTH DYNAMICS IN 3D POROUS MEDIA

GEORGE E. KAPELLOS[*], TERPSICHORI S. ALEXIOU[*†], STAVROS PAVLOU[*†]

[*] Department of Chemical Engineering
University of Patras
Karatheodori Str. 1, GR-26504, Patras, Greece
E-mail: gek222@chemeng.upatras.gr, xalexiou@chemeng.upatras.gr, sp@chemeng.upatras.gr
www.chemeng.upatras.gr

[†] Institute of Chemical Engineering & High Temperature Chemical Processes (ICEHT)
Stadiou Str., Platani, GR-26504, Patras, Greece
www.iceht.forth.gr

Key words: Multiscale Modeling; Biofilm Dynamics; Porous Materials; Fluid-Biofilm Interactions.

Abstract. Recently, we developed the first hierarchical, hybrid simulator for the prediction of the pattern of evolution and the rate of growth of heterogeneous biofilms within the pore space of porous media [*Kapellos et al., Adv. Water Resour. (2007) 30:1648-1667*]. An improved version of our simulator is presented in this work. A continuum-based approach for fluid flow and solute transport is combined with individual-based approaches for biofilm growth, detachment, and migration in the pore space. The Navier-Stokes-Brinkman equations are solved numerically with a marker-and-cell finite difference scheme to determine the velocity and pressure fields in the pore space. Momentum transport in the biofilms is described in the context of biphasic poroelasticity and a Galerkin finite element method is used to determine the solid stress field. Shear-induced biofilm detachment is taken into account explicitly and a Lagrangian-type simulation is used to determine the trajectories of detached fragments. Nutrient transport in the pore space is described by the convection-diffusion-reaction equation, which is solved numerically with an operator-splitting finite difference scheme. Further, a novel, physically-constrained cellular-automaton model is used for biofilm proliferation. As an example application, the simulator is used to investigate the impact of biofilm formation on the fate and transport of suspended particles in a network of three-dimensional pores.

1 INTRODUCTION

In nature most microbial cells are able to attach, grow and eventually form biofilms at the interface between an aqueous phase and another fluid, solid or even porous material, if favorable local environmental conditions persist. The term biofilm is used to describe a microbial consortium dispersed in a matrix of extracellular polymeric substances (EPS), and attached on a surface [1]. The EPS are mainly polysaccharides and proteins, which are either

actively secreted by the microbial cells or accumulate in the extracellular space after cell lysis. The EPS matrix serves several functions including cohesiveness between neighboring cells, structural integrity of the entire biofilm, protection from predation, antimicrobials, and others [2]. The ability of certain biofilm-forming microbial species to degrade detrimental (or synthesize useful) chemical species is driving the interest of scientists and engineers in studying and developing techniques based on microbial biofilms. For example, this ability of microbes is observed during the natural attenuation of contaminants dissolved in the groundwater, and is exploited during the treatment of contaminated and waste water in porous medium based bioreactors (e.g., packed and fluidized beds, hollow-fiber membranes).

Porous media are exquisite *hosts* for biofilm-forming bacteria because of their high specific surface [3]. The analysis of biofilm growth in porous media is not trivial since the structure of the system exhibits a *hierarchy of characteristic length scales* that spans several orders of magnitude (from several nanometers in the EPS up to a few hundreds of meters at the aquifer scale – Fig. 1) and, further, there exists an intricate interplay of hydrodynamic, physico-chemical and biological processes occurring at different *characteristic time scales*. In addition, each structural level might be heterogeneous with respect to geometrical and topological characteristics (e.g. pore and grain size, shape and connectivity), physical properties (e.g. fluid density and viscosity), chemical composition (e.g. mineralogy of the solid matrix), as well as biological composition and activity (e.g. number and physiological state of bacterial cells). A generic description of the main processes involved in the formation of biofilms in porous media is given in [4].

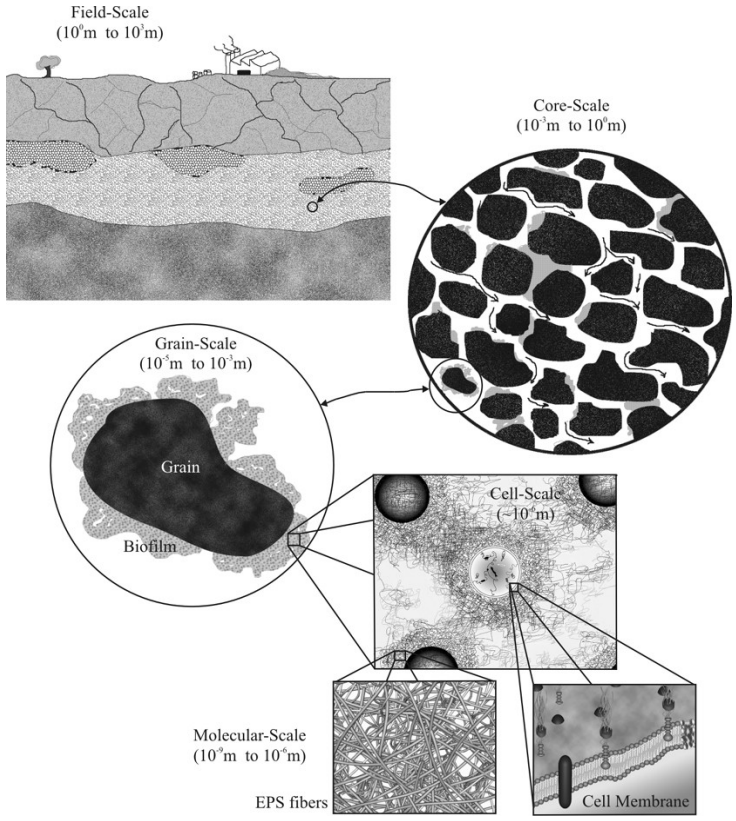

Figure 1: Biofilms in porous media: hierarchical structure of the system (reprinted from [4]).

Mathematical models and simulators are indispensable tools for the study of such complex systems because these can be used to postulate and test hypotheses concerning the underlying mechanisms, to design and interpret experiments, and to optimize the performance of bioreactors. Up to date, significant work has been devoted in the development of models for this process on a single length scale (e.g., biofilm or field scale), neglecting what happens at smaller and/or larger length scales. However, the process under consideration is inherently multiscale, meaning that the different length scales interact strongly to produce the observed behavior. For example, the pressure drop and the residence time distribution of dissolved or particulate matter, which are typically measured at the reactor-scale depend strongly on the detailed spatial distribution of the biofilms at the core-scale.

We have recently developed the first hierarchical, hybrid computer simulator of biofilm growth dynamics in porous media (HiBioSim-PM) [4]. The simulator predicts: i) the structural and biological heterogeneity at the biofilm scale, and ii) the pattern of evolution and the rate of growth of heterogeneous biofilms within the pore space of porous media (core scale). A continuum-based approach for fluid flow and mass transport is combined with individual-based approaches for biofilm growth, detachment, and migration in the pore space. The rationale for the development of this *hybrid* approach is the disparity in characteristic lengths between chemical species and biofilms. Mesoscopic cooperative effects are taken into account explicitly, and the impact of biofilm formation on the spatiotemporal distribution of preferential flowpaths and concentration profiles of dissolved substances is determined. In this work, we present an improved version of our simulator and use it to investigate the impact of biofilm formation on the fate and transport of colloidal particles in a three-dimensional model pore structure.

2 DESCRIPTION OF THE SIMULATOR (HIBIOSIM-PM)

A brief description of the main modules of the simulator is given in the following paragraphs, and more details can be found in [4,5].

2.1 Generation of the pore structure

In the present work, a planar network of three-dimensional pores with rhombohedral topology is used as a model pore structure. This type of porous medium was selected because it models the microfluidic pore networks used in our laboratory for experimental studies of biofilm formation. In general, any type of computer-generated virtual structure, or digitized representations of real porous media can be used in the simulator. In previous works, we have used unconsolidated and consolidated cores of granular porous media [4-6].

2.2 Inoculation of the pore structure

The inoculation sites are determined as follows. First, the flow field within the pore space is determined as described in subsection §2.5. Then, a single microbial cell at a time is inserted randomly at the inflow boundary of the virtual porous medium and moves along the streamlines (§2.6) until it is captured at a grain surface or exits the system. This procedure is repeated until the number of initially attached microbial cells (*first colonists*) equals a prescribed value.

2.3 Biofilm growth

With regard to the biological processes, the biofilm is treated as a population of interacting individual microbial cells, which consume nutrients, grow, proliferate, and synthesize EPS. The growth and proliferation of microbial cells within the biofilm is modeled using a 3D cubic lattice of unit biomass compartments (UBCs). A UBC might contain a single microbial cell (single occupancy UBC) or more than one microbial cells of the same species (multiple occupancy UBC). A state vector is assigned to each UBC. The state vector contains information about the species (for mixed biofilms), the size, and the physiological status (active, dormant or apoptotic) of the microbial cell that occupies the UCB, as well as the volume fraction and the porosity of the EPS hydrogel. The active microbial cells assimilate nutrients and synthesize new cellular mass with rate proportional to their mass. Part of the cellular mass is used for maintenance purposes (endogenous metabolism). Simultaneously, they synthesize and secrete EPS within their UBC with rate proportional to their growth rate. Part of the EPS matrix lyses (say due to enzymatic or hydrolytic action) with rate proportional to its mass. Based on these assumptions the mass balances for bacterial cells and EPS within a UBC are

$$\frac{dX_{\kappa}}{dt}=\mu_{\kappa,g}X_{\kappa}-\mu_{\kappa,m}X_{\kappa} \tag{1}$$

$$\frac{dX_{\pi}}{dt}=Y_{\pi/\kappa}\mu_{\kappa,g}X_{\kappa}-k_{lys}X_{\pi} \tag{2}$$

where X_{κ}, X_{π} denote the mass of cells, EPS over the volume of a UBC, and $\mu_{\kappa,g}$, $\mu_{\kappa,m}$, $Y_{\pi/\kappa}$, k_{lys} are kinetic parameters, which might be defined as functions of the local environmental conditions (nutrient concentrations, mechanical stresses, temperature, pH, etc.). For the simulation results presented in this work we used the following expression for the local specific growth rate of cells

$$\mu_{\kappa,g}=F_n(C_n)F_{\sigma}(I_{\beta}) \tag{3}$$

$$F_n(C_n)=\mu_{max}\frac{C_n}{K_C+C_n} \tag{4}$$

$$F_{\sigma}(I_{\beta})=\begin{cases}1-I_{\beta}/I_{\beta,crit} & if\ I_{\beta}\leqslant I_{\beta,crit}\\ 0 & otherwise\end{cases} \tag{5}$$

Here, C_n is the local concentration of a growth-limiting nutrient, I_{β} is the first invariant of the local stress tensor for the solid components of the biofilm, and μ_{max}, K_C, $I_{\beta,crit}$ are kinetic parameters.

If the specific growth rate is greater than a critical value, $\mu_{\kappa,g,crit}$, the active bacterial cells continuously increase their mass until it exceeds a prescribed upper threshold value, $m^{+}_{\kappa,crit}$. Then they divide into two equal daughter cells (the number of cells within the UBC doubles and the mass of each cell halves). If the specific growth rate gets lower than the critical value, the cells enter the dormancy state during which the metabolic activity is halted and only consumption of cellular mass for maintenance purposes takes place. Dormant cells may be activated once again if the specific growth rate is restored to a value greater than the critical.

During dormancy, cellular mass decreases continuously until a prescribed lower threshold value, $m_{\kappa,crit}^{-}$, is reached. Then the cells enter the apoptosis state (programmed cell death), which is irreversible and lysis of the cells occurs with probability

$$p_{ap}(\tau_{ap}) = 1 - \exp(-k_{ap}\tau_{ap}) \tag{6}$$

where τ_{ap} is the time since the cells became apoptotic and k_{ap} is the apoptosis rate constant.

2.4 Cell proliferation and EPS spreading

The microbial cells move within the biofilm because of the internal stresses that develop during the division of cells. In this work, the cellular motion that is caused by cell divisions is modeled on the 3D cubic lattice of UBCs, by implementing a least-action principle. In particular, if the mass of a cell exceeds a corresponding, prescribed maximum value then *biomass percolates* from the UBC, which is occupied by the cell under division, towards the nearest empty-UBC, which contains only fluid and/or EPS hydrogel, along the *path that minimizes the energy of displacement.* First, a random walk procedure is used to generate a large number of paths that connect the UBC, which is occupied by the cell under division, and the nearest empty-UBC, without passing over solid obstacles. Then, the shortest of them is chosen. If there are more than one paths with the same minimum length, then the path that corresponds to the minimum EPS content is chosen. Afterwards, the overgrown UBC displaces its adjacent UBC (defined by the path) and thus generates a temporarily empty-UBC in which it puts half of its biomass, while it retains the other half. The displaced UBC in turn displaces its adjacent UBC and takes its position. This sequence of interactions continues until the end position of the path.

2.5 Fluid flow and fluid-biofilm interaction

With regard to momentum and mass transport processes, the biofilm is treated as a biphasic *continuum* with poroelastic material behavior. Single-phase flow of an incompressible Newtonian fluid (say a dilute aqueous solution) is considered within the pore space of the porous medium, which is occupied partly by fluid and partly by biofilms. Within the fluid regions, the Navier-Stokes equations and the continuity equation result from the formulation of the momentum and mass balance, respectively. Within the porous biofilm, Brinkman's extension of Darcy's law is considered as an appropriate equation to describe the flow along with the conservation of total fluid mass. Further, linear elastic behavior is considered for the solid components of the biofilm [7]. The final equations are

$$\nabla \cdot \mathbf{v}_f = 0 \tag{7}$$

$$\rho_f \frac{\partial \mathbf{v}_f}{\partial t} + \alpha_c \rho_f \nabla \cdot (\mathbf{v}_f \mathbf{v}_f / \varepsilon_\beta) = -\varepsilon_\beta \nabla P_f + \mu_f \nabla^2 \mathbf{v}_f - (1-\alpha_c)\varepsilon_\beta \frac{\mu_f}{k_\beta} \mathbf{v}_f \tag{8}$$

$$\mathbf{0} = \nabla \cdot \boldsymbol{\sigma}_s + \mathbf{F}_{f \to s} \tag{9}$$

$$\boldsymbol{\sigma}_s = -(1-\varepsilon_\beta) P_f + \lambda_s (\nabla \cdot \mathbf{u}_s) + \mu_s [\nabla \mathbf{u}_s + \mathbf{u}_s \nabla] \tag{10}$$

$$\mathbf{F}_{f \to s} = \varepsilon_\beta \frac{\mu_f}{k_\beta} \mathbf{v}_f \tag{11}$$

Here, $\mathbf{v}_f$ is the local superficial velocity of the fluid, P_f is the intrinsic pressure of the fluid, $\mathbf{u}_s$ is the local displacement of the solids in the biofilm, μ_s, λ_s are the Lamé parameters for the solid, μ_f is the fluid viscosity, ρ_f is the fluid density, ε_β is the local volume fraction of fluid, k_β is the local hydraulic permeability (defined only within the regions of porous biofilms) and α_c is a computational parameter that equals unity within regions of fluid and zero within biofilms. The local hydraulic permeability of the biofilm is calculated as a function of the volume fractions of cells, EPS and water, the average diameter of cells, the average diameter of EPS fibers, and the internal porosity of the EPS (see Appendix in [4]).

Equations (7) and (8) are valid everywhere in the pore space (fluid and biofilm regions), while equation (9) applies only in the biofilm regions. These equations are solved numerically by combining finite difference and finite element methods as follows. First, eqs.-(7),(8) are solved numerically using a staggered grid for the spatial discretization, central finite differences for the viscous and pressure terms and a higher-order upwinding scheme for the inertial terms. Then, eq.-(9) is solved using the Galerkin finite element method on a structured mesh of hexahedral elements with C0-quadratic interpolation functions for the displacement.

2.6 Detachment, migration, and reattachment

If a UBC is adjacent to clear fluid, the average shear stress acting on the surfaces exposed to fluid is calculated. Then, if the exerted shear stress exceeds a designated critical value, the UBC is considered to loose the cohesiveness with adjacent UBCs or solid surfaces. Afterward, the UBC begins to move along the fluid streamlines as if a fluid element (in a first approximation the effects of gravity and drag forces are neglected based on the facts that biofilm is highly porous and its density is very close to that of the aqueous solution). The trajectory of the UBC within the pore space is calculated from the numerical integration of

$$\frac{d\,\mathbf{r}_p}{dt} = \mathbf{v}_f \tag{12}$$

where $\mathbf{r}_p$ is the position of the mass center of the UBC at time t. The UBC stops moving if it passes over the outflow boundary of the porous medium or if it becomes reattached to grain or biofilm surface, which is exposed to shear stress lower than the critical value. If at least one UBC has been detached, the flow field is updated.

2.7 Solute transport

The fate of a dissolved substance 'A' (nutrient, chemical signal etc.) is determined from the convection-diffusion-reaction equation

$$\frac{\partial}{\partial t}(K_{A,\beta/f}\, C_A) + \nabla\cdot(\mathbf{v}_f\, C_A) = \nabla\cdot[\mathbf{D}_{A,eff}\cdot\nabla C_A] + R_A \tag{13}$$

where C_A is the concentration, $K_{A,\beta/f}$ is the partition coefficient between the biofilm and the aqueous solution, $\mathbf{D}_{A,eff}$ is the local effective diffusivity and R_A is the local reaction rate of the dissolved substance A. The diffusion coefficient in the biofilm is calculated using the recently developed model in [8]. Equation (7) is solved using a fractional step method, in which the solution procedure is split up into independent steps corresponding to the

convection, diffusion and reaction processes and each step is solved independently. An explicit in time, higher-order upwinding scheme is used for the convective terms, implicit central differencing is used for the diffusive terms and the explicit fourth order Runge-Kutta method is used for the reaction terms.

3 RESULTS AND DISCUSSION

Here, we present sample simulation results of biofilm growth in a pore network with rhombohedral topology. The values of the physicochemical, biological and operational parameters used in this simulation are the same with those used in [4]. Figure 2 shows snapshots of the spatiotemporal evolution of biofilms within the pore space, at various points in time. Initially, small biofilms are formed at the sites of inoculation. Thereafter, the initial biofilms grow further and, also, new colonies appear downstream. These new colonies are formed by the re-attachment of cells that detached from biofilms near the inflow boundary. By the time, the biofilms grow, spread, merge, and cover completely the surface of pores. Under conditions of constant flow rate through the pore network, the reduction of the clear pore sections results in increased fluid velocities which, in turn, cause increased shear stresses at the fluid-biofilm interface. High shear stresses cause continuous erosion of the biofilm surface and, thus, maintain the pores unplugged (in this simulation).

The impact of biofilm formation on the fate and transport of colloidal particles is determined via the following computer experiment. For a given configuration of biofilms, we perform particle tracking for a large number, typically one million, of particles. As a first approximation, we considered that the drag force, which is exerted by the fluid on the particle, is dominant in the force balance and, thus, the trajectory of each particle can be determined from the numerical solution of Eq.-(12). Every particle enters at a random position of the inflow boundary and moves until either it passes over the outflow boundary, or it is captured by interception at the fluid-solid or fluid-biofilm interface. Figure 3 shows the residence time distributions of particles convected out of the pore network for six different spatial configurations of biofilms, and for two different scenarios regarding the flow through the biofilms: a) impermeable biofilms (k_β=0), and b) permeable biofilms (k_β=10μm^2). Further, Fig.-4A shows the effect of the biofilm volume fraction on the average residence time of particles, which are convected out of the pore network. Two important observations can be made. First, as the amount of biofilms increases, the residence time distribution changes form, narrows, and moves to lower values of particle residence time. This trend was intuitively expected because the fluid velocity in the pores increases as the clear pore section decreases. Second, for a given configuration of biofilms, even imperceptible flow through the biofilms results in decreased fluid velocities in the clear pore regions and, thus, in longer residence times for the particles.

A very interesting behavior is observed with regard to the effect of the biofilm volume fraction on the removal efficiency of particles, which is shown in Fig.-4B. As the amount of biofilm increases up to a certain value, the percentage of captured particles increases monotonically. Beyond that value, further increase in the biofilm volume fraction doesn't affect the particle removal efficiency substantially. This behavior is explained as follows. The initial formation of irregular biofilm colonies increases the available area for particle deposition and, thus, results in increased particle removal efficiency. However, at later stages

of the process, the available area for particle deposition decreases again because the biofilms cover completely the surface of the pores and, further, the fluid-biofilm interface becomes smooth by the action of increased shear stress. Nonetheless, the particle removal efficiency doesn't undergo substantial change because the effect of decreased surface area is counterbalanced by the decrease in the cross section of the clear pore, which results in increased probability for a particle to obtain a limiting trajectory that leads to capture.

In Fig.-4B, we observe also that more permeable biofilms produce significantly higher removal efficiencies of particles. This is explained as follows. Higher biofilm permeability results in increased slip velocity at the fluid-biofilm interface, which allows more particles to approach closer to the interface and, thus, be captured.

4 CONCLUSIONS

- The re-attachment of detached cells and biofilm fragments enhances significantly the downstream migration of biofilms in the porous medium. This is the only computer simulator that accounts explicitly for the fate of detached biofilm fragments. In *all* previous models and simulators of biofilm formation, the detached material is merely treated as "lost".
- The formation of biofilms alters the geometrical and topological characteristics of the pore structure and the flow field, which in turn strongly affect the fate of moving particles within the porous medium. In particular, biofilm formation results in increased removal efficiency and decreased residence time of particles in the porous medium.

REFERENCES

[1] Costerton, J.W., Lewandowski, Z., de Beer, D., Caldwell, D., Korber, D. and James, G. Biofilms, the customized microniche. *J. Bacteriol.* (1994)176:2137-2142.

[2] Rittmann, B.E. The significance of biofilms in porous media. *Water Resour. Res.* (1993) 29(7):2195-202.

[3] Wolfaardt, G.M., Lawrence, J.R. and Korber D.R. "Function of EPS." In: Wingender, J., Neu, T.R. and Flemming H.-C. (Eds.) Microbial Extracellular Polymeric Substances: characterization, structure, and function. Springer-Verlag (1999) pp.171-200.

[4] Kapellos, G.E., Alexiou, T.S. and Payatakes A.C. Hierarchical simulator of biofilm growth and dynamics in granular porous materials. *Adv. Water Resour.* (2007)30:1648-67.

[5] Kapellos G.E. Transport phenomena and dynamics of microbial biofilm growth during the biodegradation of organic pollutants in porous materials: hierarchical theoretical modeling and experimental investigation. Doctoral thesis in Greek. (2008) http://nemertes.lis.upatras.gr/dspace/handle/123456789/1693

[6] Kapellos G.E., Alexiou T.S., Pavlou S. and Payatakes A.C. Hierarchical simulation of biofilm growth dynamics in porous media. In: Starrett, S.K. et al. (Eds.) *Environmental Science and Technology*, American Science Press, Houston, USA, Vol. 1, (2007) 491-502.

[7] Kapellos, G.E., Alexiou, T.S. and Payatakes A.C. Theoretical modeling of fluid flow through cellular biological media: An overview. *Math. Biosci.* 225(2):83-93 (2010).

[8] Kapellos, G.E., Alexiou, T.S. and Payatakes A.C. A multiscale theoretical model for diffusive mass transfer in cellular biological media. *Math. Biosci.* (2007) 210(1):177-237.

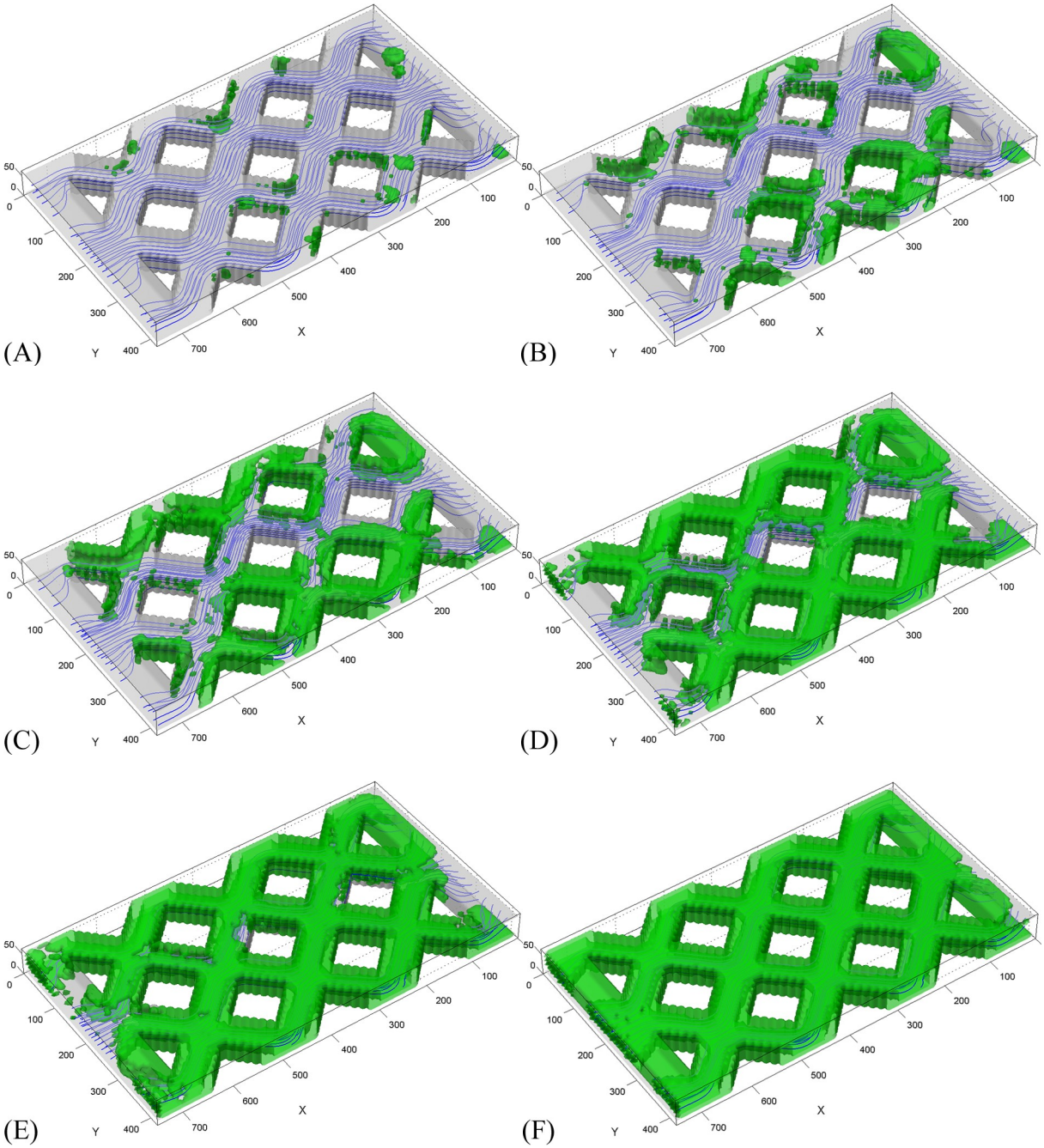

Figure 2: Spatial distribution of biofilms within the pore space at various time instants: (A) t^*=7, (B) t^*=12, (C) t^*=15.5, (D) t^*=20.5, (E) t^*=24.25, (F) t^*=30, where $t^*=\mu_{max}t$ and μ_{max} is the specific growth rate of cells.The blue lines are equidistant streamlines. The biofilms (green color) and the pore space (gray color) are semi-transparent for better visualization.

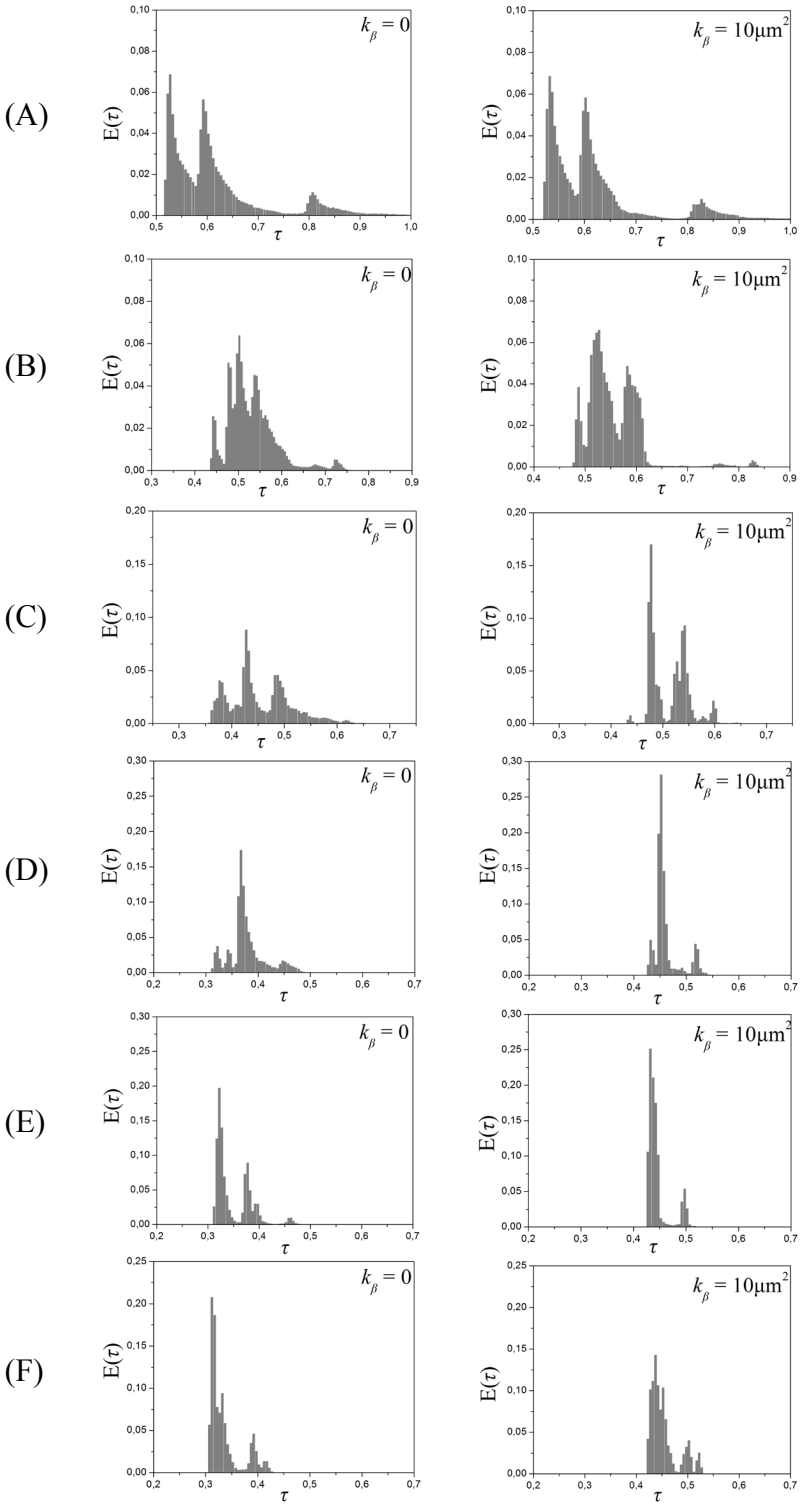

Figure 3: Residence time distributions of particles convected out of the pore network for two scenarios: impermeable biofilms (left column, k_β=0), and permeable biofilms (right column, k_β=10μm^2). The capital letters on the outer left denote the corresponding biofilm distributions shown in Figure 2.

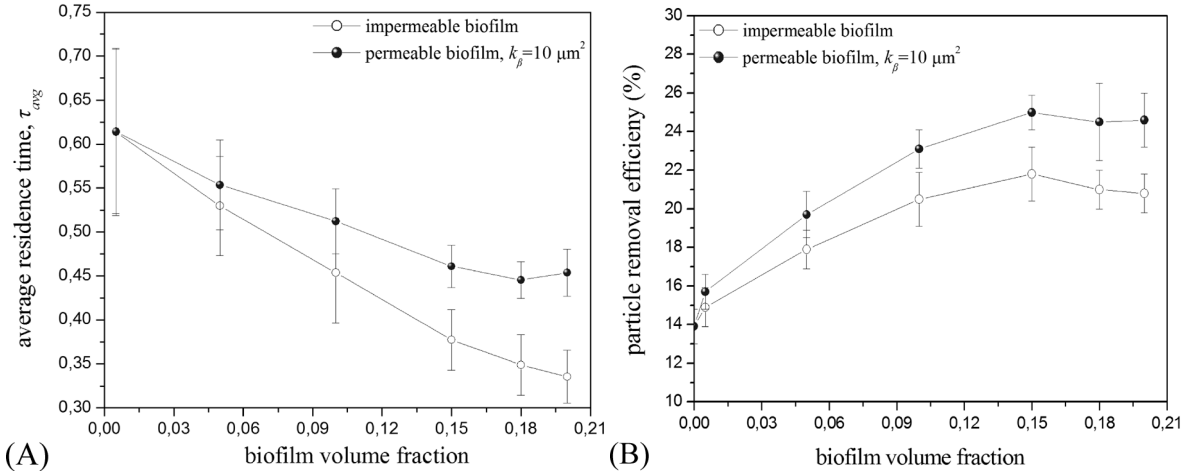

Figure 4: Impact of the biofilm volume fraction on: (A) the average residence time of particles convected out of the pore network, and (B) the efficiency of particle removal (i.e., percentage of captured particles).